Magnetic Resonances and Susceptibility in Orthoferrites*

GABRIEL F. HERRMANN
Lockheed Research Laboratories, Palo Alto, California
(Received 25 September 1963)

Magnetic resonances and susceptibilities are calculated for various allowed magnetic structures in orthoferrites and similar magnetic perovskites. The calculation is based on a general form for the free energy which includes canting contributions from both single-ion anisotropy and antisymmetric exchange, and which assumes four distinct interacting magnetic sublattices. The results are compared with those obtained from a simplified 2-sublattice model, and the effect of hidden canting on overt behavior is evaluated. When antisymmetric exchange is the predominant canting mechanism, a 2-sublattice model presents a correct formal (but not necessarily physical) picture for the antiferromagnetic resonance modes and for low-frequency magnetic behavior, provided that exchange effects associated with hidden canting are properly incorporated within an effective anisotropy energy. This effective anisotropy will, in general, not have the physical properties, e.g., temperature dependence, typical of single-ion anisotropy. A 4-sublattice model is required for the analysis of the high-frequency exchange modes. It is found that these modes are coupled by the spin canting mechanism to the antiferromagnetic modes and as a result become optically active. In general, one finds that, of the many interaction coefficients possible in a 4-sublattice system, only relatively few can be determined by direct macroscopic measurement.

I. INTRODUCTION

ORTHOFERRITES are typical representatives of a class of magnetic materials which crystalize in a slightly distorted perovskite structure of orthorhombic symmetry. In many instances these substances are canted antiferromagnets[1] and exhibit on the macroscopic scale some of the detailed structural aspects of the superexchange mechanism. They are also of interest as examples of multisublattice systems which possess several optically active magnetic resonance modes. The orthoferrites, in the strict sense, are mixed oxides of composition $M\mathrm{FeO_3}$, where M is a trivalent metal. We shall, however, use the term generically to include other magnetic substances of isomorphic structure, e.g., the orthomanganites, or more remotely related, $\mathrm{KMnF_3}$ in its orthorhombic phase. The present analysis is confined to those cases where the metallic ion M is nonmagnetic. The more general and much more complicated case, in which two distinct magnetic species are present, will merit a separate discussion.

The structure of orthoferrites has been studied in detail by Geller[2] and associates and by Bertaut and Forrat,[3] and there exist in the literature several visual representations of this rather involved crystalographic configuration.[2,4] For our purpose, Fig. 1 which indicates the location of the Fe ions in the unit cell will suffice. There are four distinct iron sublattices, with an approximately antiferromagnetic arrangement of nearest-neighbor spins.[5] In the present convention, sublattices 1 and 3 are oriented in one direction, and sublattices 2 and 4 in the opposite one. Canting is exhibited as a small deviation of the sublattice magnetization vectors from strict antiferromagnetic allignment and can assume various forms (Fig. 2). In general one can distinguish two types of canting. The first which we shall call overt, consists in a bending of the spins toward a direction perpendicular to the axis of ferromagnetism and gives rise to a small resultant ("residual") magnetization. This phenomenon is commonly referred to as "weak ferromagnetism."[6] In the second type, which we shall refer to as hidden canting, the spins fan out symmetrically about the axis and produce no resultant magnetization. As a rule, both types exist side by side, but while overt canting is directly observable, the influence of hidden canting is largely indirect.

The physical origin of canting may be found either in the magnetic anisotropy of the individual ion site, or in an antisymmetric exchange interaction of the form $\mathbf{D}\cdot\mathbf{S}_1\times\mathbf{S}_2$, first postulated by Dzialoshinski,[7] and later derived theoretically by Moriya.[8] According to Treves,[9] antisymmetric exchange is the predominant cause of canting in several orthoferrites. In $\mathrm{KMnF_3}$, on the other hand, it would seem that single-ion anisotropy

* This work is supported by the Lockheed Independent Research Fund.

[1] R. M. Bozorth, Phys. Rev. Letters **1**, 362 (1958).

[2] S. Geller and E. A. Wood, Acta Cryst. **9**, 563 (1956); S. Geller and V. B. Bala, *ibid.* **9**, 1019 (1956); M. A. Gilleo, *ibid.* **10**, 161 (1957); S. Geller, *ibid.* **10**, 243 (1957); **10**, 248 (1957); S. Geller, J. Chem. Phys. **24**, 1236 (1956); G. Geller, Acta Cryst. **9**, 885 (1956).

[3] F. Bertaut and F. Forrat, J. Phys. Radium **17**, 129 (1956).

[4] A. J. Heeger, O. Beckman, and A. M. Portis, Phys. Rev. **123**, 1652 (1961).

[5] W. C. Koehler and E. O. Wollan, Phys. Chem. Solids **2**, 100 (1957); W. C. Koehler, E. O. Wollan, and M. K. Wilkinson, Phys. Rev. **118**, 58 (1960).

[6] R. Pauthenet and P. Blum, Compt. Rend. **239**, 33 (1954); H. Forestier and G. Guiot-Guillain, *ibid.* **230**, 1844 (1957); M. A. Gilleo, J. Chem. Phys. **24**, 1239 (1956); R. M. Bozorth, V. Kramer, and J. P. Remeika, Phys. Rev. Letters **1**, 3 (1958); R. C. Sherwood, J. P. Remeika, and H. J. Williams, J. Appl. Phys. **30**, 217 (1959); H. Watanabe, J. Phys. Soc. Japan **14**, 511 (1959); C. Kuroda, T. Miyadai, A. Naemura, N. Niizeki, and H. Takata, Phys. Rev. **122**, 466 (1961); G. H. Jonker, Physica **22**, 707 (1956).

[7] I. Dzialoshinski, Zh. Eksperim. i Teor. Fiz. **32**, 1547 (1957) [English transl.: Soviet Phys.—JETP **6**, 1130 (1958)]; Phys. Chem. Solids **4**, 241 (1958).

[8] T. Moriya, Phys. Rev. **120**, 91 (1960).

[9] D. Treves, Phys. Rev. **125**, 1843 (1962).

predominates.[4] It has been shown that the two canting interactions produce distinguishable magnetic behavior[9,10] and should not in general be lumped together.

The existence of four distinct sublattices makes the task of relating macroscopic phenomena to microscopic effects rather complicated, because of the large number of possible interaction parameters. In previous studies,[9,10] the analysis was greatly simplified by resorting to a 2-sublattice model in which the respective sublattice pairs (1,3) and (2,4) were each represented by a single magnetization vector, thereby eliminating at one blow a majority of the interaction parameters. The physical assumption implicit in this model is that all hidden canting effects can be ignored. As we shall see below, this model is very useful at low frequencies in important special cases, provided the proper physical interpretation is given to the constants used. Nevertheless, as shown by Joenk[11] in the related case of $CuCl_2 \cdot 2H_2O$, important details are lost in this approximation, particularly with respect to magnetic behavior at higher frequencies, as reflected in the optical activity of the exchange modes.

In the following sections we present a detailed analysis of the macroscopic dynamics of the magnetic system in orthoferrites, based on a full 4-sublattice model. In particular, expressions are derived for equilibrium configurations, residual magnetization, and equilibrium energy for the various allowed magnetic structures. Precession modes are analyzed in detail and expressions are found for the various resonances, for mode amplitudes, and for the high-frequency susceptibility (from which the dc susceptibility is obtained as a special case). The approach used in the calculation is fairly general, in that it includes canting contributions both from single-ion anisotropy and from exchange, and on the whole avoids approximations based on heuristic arguments. From the number of independent interaction constants one may immediately conclude that the task of relating theory and experiment is a formidable one which requires, on the one hand, information from many diverse types of experiments, and, on the other hand, a very detailed theory. One of the objectives of the present calculation has therefore been to define the "measurable parameters" of the problem, i.e., those parameters which can be definitively established in a given experiment, and determine which, if any, of the macroscopic phenomena are uniquely related to a specific microscopic interaction. In particular we investigate the effect of hidden canting on overt behavior and establish the relation of the 4-sublattice dynamic model to the 2-sublattice model. Since the latter model has the virtue of simplicity its continued use by workers in the field is likely, and it is important to establish its range of validity and limitations.

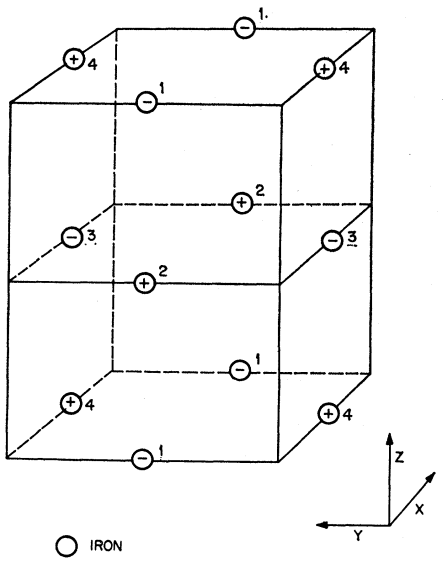

FIG. 1. Unit cell of the orthorhombic orthoferrite showing and indexing the iron sites.

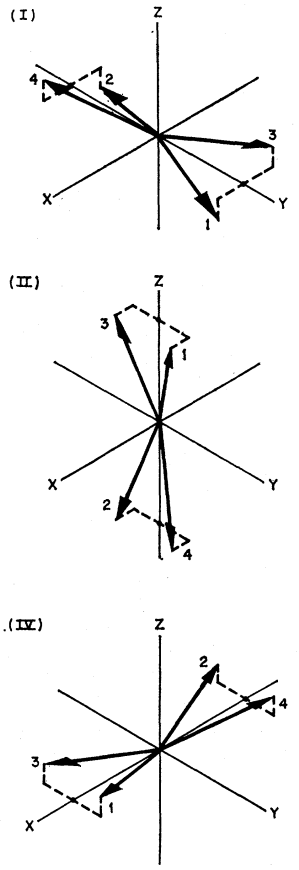

FIG. 2. Allowed magnetic configurations in orthoferrites. Configuration III, which is incompatible with the antiferromagnetic interaction, is not shown.

II. CRYSTAL STRUCTURE AND THE MAGNETIC CONFIGURATIONS

Orthoferrites belong to the crystallographic point group D_{2h} and to the space group $D_{2h}^{16}-D_{bnm}$. In

[10] G. F. Herrmann, Phys. Chem. Solids **24**, 597 (1963).
[11] R. J. Joenk, Phys. Rev. **126**, 565 (1962).

dealing with fundamental precession the displacement operations of the space group are irrelevant, since they merely transform each sublattice into itself. Each point group operation produces, on the other hand, a permutation among the four iron sublattices, e.g., the 2-fold rotation about x results in the permutation (14)(23). Proper combinations of permutations and point group operations can therefore serve as elements of the symmetry group. Moreover, since each Fe site is a center of inversion, it suffices to consider the elements E, C_{2x}, C_{2y}, C_{2z} of the smaller point group D_2. The required symmetry group is given by E, $C_{2x}(14)(23)$, $C_{2y}(13)(24)$, $C_{2z}(12)(34)$ where the 2-fold rotations C_{2x}, C_{2y}, C_{2z} may be regarded as orthogonal transformations acting on the magnetization vectors, and the associated permutations as acting on the subscripts denoting the respective sublattices.

The magnetic structure and interactions in orthoferrites are discussed in detail by Bertaut.[12] The equilibrium spin configuration must belong to one of the magnetic groups derived from the crystallographic point group. The magnetic groups can be obtained by the method of Tavger and Saitzev[13] by appending the time reversal operator R to D_2. In the case of orthoferrites there is no reason to expect that the inclusion of spins will result in an inherent reduction of the symmetry. One arrives at four "complete" magnetic groups, and correspondingly four magnetic structures as follows:

configuration I (E,C_{2x},C_{2y},C_{2z});

$$M_{1x}=-M_{2x}=-M_{3x}=M_{4x},$$
$$M_{1y}=-M_{2y}=M_{3y}=-M_{4y},$$
$$M_{1z}=M_{2z}=-M_{3z}=-M_{4z},$$

configuration II $(E,C_{2x},RC_{2y},RC_{2z})$;

$$M_{1x}=M_{2x}=M_{3x}=M_{4x},$$
$$M_{1y}=M_{2y}=-M_{3y}=-M_{4y},$$
$$M_{1z}=-M_{2z}=M_{3z}=-M_{4z},$$

configuration III $(E,RC_{2x},C_{2y},RC_{2z})$;

$$M_{1x}=M_{2x}=-M_{3x}=-M_{4x},$$
$$M_{1y}=M_{2y}=M_{3y}=M_{4y},$$
$$M_{1z}=-M_{2z}=-M_{3z}=M_{4z},$$

configuration IV $(E,RC_{2x},RC_{2y},C_{2z})$;

$$M_{1x}=-M_{2x}=M_{3x}=-M_{4x},$$
$$M_{1y}=-M_{2y}=-M_{3y}=M_{4y},$$
$$M_{1z}=M_{2z}=M_{3z}=M_{4z},$$

where $\mathbf{M}_i$ is the magnetization vector for sublattice i.

In orthoferrites the interaction between nearest neighbors, i.e., sublattices 1 and 2, 1 and 4, 2 and 3, and 2 and 4, is essentially antiferromagnetic.[5] Configuration III is therefore ruled out as a ground state. The remaining configurations are represented schematically in Fig. 2. In configuration I the spins are essentially along the y direction, and there is no overt canting. In configuration II the spins are essentially along the z direction with a residual component of magnetization along x. In configuration IV the spins lie essentially along the x direction with residual magnetization along z.

Each configuration exists in two types of domains. In cases II and IV these will correspond to opposite residual magnetizations. In I, which has no magnetization, the domains may be characterized as right or left handed, respectively.

III. FREE ENERGY AND DYNAMIC EQUATIONS

We consider four types of contributions to the free energy of the magnetic system. The first, and by far largest, contribution is made by isotropic exchange interactions. These are denoted by E with appropriate subscripts denoting the sublattices involved. Next is antisymmetric exchange, with coefficients D, and the single-ion anisotropy, A. Last there is the interaction with an applied field $\mathbf{H}$. Symmetric anisotropic exchange is not included at present, and only quadratic terms are included in the single-ion anisotropy energy (see Sec. IV for a discussion of these omissions). As usual it is assumed that $M_1=M_2=M_3=M_4$, where M remains a constant during precession.

It will be convenient to work throughout in units of magnetic field. Instead of the free energy F, we use the normalized magnitude $V=F/M$, and define unit directional vectors

$$\mathbf{r}_i=\mathbf{M}_i/M$$

with components (x_i,y_i,z_i) to describe the sublattice magnetization vectors.

The most general form for V, compatible with symmetry, is

$$\begin{aligned}V=&E_{12}(\mathbf{r}_1\cdot\mathbf{r}_2+\mathbf{r}_3\cdot\mathbf{r}_4)+E_{13}(\mathbf{r}_1\cdot\mathbf{r}_3+\mathbf{r}_2\cdot\mathbf{r}_4)+E_{14}(\mathbf{r}_1\cdot\mathbf{r}_4+\mathbf{r}_2\cdot\mathbf{r}_3)+D_{12x}(y_1z_2-y_2z_1-y_3z_4+y_4z_3)\\&+D_{12y}(z_1x_2-z_2x_1+z_3x_4-z_4x_3)+D_{13x}(y_1z_3-y_3z_1-y_2z_4+y_4z_2)+D_{13z}(x_1y_3-x_3y_1+x_2y_4-x_4y_2)\\&+D_{14y}(z_1x_4-z_4x_1-z_2x_3+z_3x_2)+D_{14z}(x_1y_4-x_4y_1+x_2y_3-x_3y_2)-A_{xx}\textstyle\sum x_i^2-A_{yy}\sum y_i^2-A_{zz}\sum z_i^2\\&-A_{xy}(x_1y_1+x_2y_2-x_3y_3-x_4y_4)-A_{yz}(y_1z_1-y_2z_2-y_3z_3+y_4z_4)-A_{zx}(z_1x_1-z_2x_2+z_3x_3-z_4x_4)-\mathbf{H}\cdot\textstyle\sum\mathbf{r}_i.\end{aligned}\quad(1)$$

The sign of some of the coefficients depends on the particular choice of sublattice labels. While this choice does not effect any of the macroscopic results, care must be used in applying it consistently.

[12] E. F. Bertaut, J. Phys. Radium **23**, 460 (1962).
[13] B. A. Tavger and V. M. Saitzev, Zh. Eksperim. i Teor. Fiz. **30**, 564 (1956) [English transl.: Soviet Phys.—JETP **3**, 430 (1956)].

In order to keep the calculation within reasonable bounds it is convenient to follow Dzialoshinski[7] and introduce a system of symmetry coordinates defined by

$$\begin{aligned} 2\mathbf{r}_O&=\mathbf{r}_1+\mathbf{r}_2+\mathbf{r}_3+\mathbf{r}_4,\\ 2\mathbf{r}_P&=\mathbf{r}_1+\mathbf{r}_2-\mathbf{r}_3-\mathbf{r}_4,\\ 2\mathbf{r}_Q&=\mathbf{r}_1-\mathbf{r}_2+\mathbf{r}_3-\mathbf{r}_4,\\ 2\mathbf{r}_R&=\mathbf{r}_1-\mathbf{r}_2-\mathbf{r}_3+\mathbf{r}_4. \end{aligned} \tag{2}$$

Apart from a constant, V is now given by

$$\begin{aligned} V=&E_O\mathbf{r}_O^2+E_P\mathbf{r}_P^2+E_R\mathbf{r}_R^2+D_x(y_Qz_P-y_Pz_Q)+D_y(z_Qx_O-z_Ox_Q)+D_z(x_Qy_R-x_Ry_Q)+(D_{12x}+D_{13x})(y_Rz_O-y_Oz_R)\\ &+(D_{12y}-D_{14y})(z_Rx_P-z_Px_R)+(D_{14z}+D_{13z})(x_Py_O-x_Oy_P)-A_{xx}(x_O^2+x_P^2+x_Q^2+x_R^2)\\ &-A_{yy}(y_O^2+y_P^2+y_Q^2+y_R^2)-A_{zz}(z_O^2+z_P^2+z_Q^2+z_R^2)-A_{yz}(y_Oz_R+y_Rz_O+y_Qz_P+y_Pz_Q)\\ &-A_{zx}(z_Ox_Q+z_Qx_O+z_Px_R+z_Rx_P)-A_{xy}(x_Oy_P+x_Py_O+x_Qy_R+x_Ry_Q)-2\mathbf{H}\cdot\mathbf{r}_O, \end{aligned} \tag{3}$$

where $E_O=E_{12}+E_{14}$, $E_P=E_{12}-E_{13}$, $E_R=E_{14}-E_{13}$, $D_x=D_{12x}-D_{13x}$, $D_y=D_{12y}+D_{14y}$, $D_z=D_{14z}-D_{13z}$. Equation (3) is obviously no shorter than (1), but it has certain distinct advantages in application, owing to the fact that most symmetry coordinates vanish at equilibrium. The new exchange coefficients represent the energy associated with bending of one particular pair of sublattice magnetization vectors relative to the other pair. E_O and D_y, which represent the energy involved in bending M_1 and M_3 against M_2 and M_4, are the only exchange parameters to appear in the 2-sublattice approximation, and together with A_{zx} are responsible for overt canting. The parameters E_P, E_R, D_x, D_z, A_{yz}, A_{xy}, are associated with various types of hidden canting. The terms associated with $(D_{12x}+D_{13x})$, $(D_{12y}-D_{14y})$, and $(D_{14z}+D_{13z})$ turn out to be unimportant for small canting angles and will not make a significant contribution to any of the final results.

The dynamic equations are given in the form

$$\dot{\mathbf{r}}_i/\gamma=\mathbf{r}_i\times\nabla_iV,$$

where the gradient ∇_i is taken with respect to the coordinates $(x_iy_iz_i)$ which are treated as independent variables, the condition $x_i^2+y_i^2+z_i^2=1$ being imposed upon completion of the operation. In order to simplify the notation, we shall set the gyromagnetic ratio γ equal to unity. This implies that all frequencies will be measured in units of magnetic field, normalized according to the true value of γ. We thus use the equation in the form

$$\dot{\mathbf{r}}_i=\mathbf{r}_i\times\nabla_iV. \tag{4}$$

IV. RESONANCE AND SUSCEPTIBILITY

In order to make best use of the available symmetry, it is best at this point to split the discussion and treat separately each of the allowed magnetic structures. We shall begin with a discussion of structure I, which is most tractable to analysis, and then apply analogous procedures to the more difficult cases of structures IV and II.

The introduction of an applied field will in general destroy the symmetry of the magnetic configuration, and therefore greatly increase the difficulty of calculation. In general one can split the magnetic field into a component compatible with the magnetic group, and a component which reverses sign upon application of some group operation. Elementary considerations indicate that the compatible component will in general produce first-order effects, while the other components produce at most second-order effects. We therefore confine ourselves to magnetic fields compatible with the magnetic groups in each configuration. We thus put $\mathbf{H}=0$ in configuration I, and take $\mathbf{H}$ along the z direction in configuration IV and along the x direction to configuration II. We make no assumption as to the direction of the small rf field $\mathbf{h}$, and can therefore still derive complete expressions for the susceptibility tensor.

In the course of the calculation it is necessary to apply drastic approximations. It is assumed that canting angles are small, and all relevant parameters are determined up to first order in the canting angle. The approximation is based on the fact that the exchange parameters E are large compared to D and A type parameters. At the same time, magnitudes of the form D^2/AE may in some instance be of the order of unity and must be retained. We therefore attempt to adhere to an approximation procedure valid for either small or large D. We retain up to quadratic terms in H, and obtain the coefficient of each power of H essentially to an accuracy comparable to the canting angles.

Configuration I

1. Equilibrium Position and Energy

Configuration I is characterized by the symmetry group $G_I=E$, $C_{2x}(14)(23)$, $C_{2y}(13)(24)$, $C_{2z}(12)(34)$. The only nonvanishing symmetry coordinates at equilibrium are x_R, y_Q, and z_P. Since the spins are essentially along the y direction one has $y_Q\sim 2$ and x_R and z_P are small. One readily obtains to first order

$$x_R=(D_z+A_{xy})/E_R, \tag{5}$$

$$z_P=-(D_x-A_{yz})/E_P, \tag{6}$$

at equilibrium. The choice of particular domain implicit

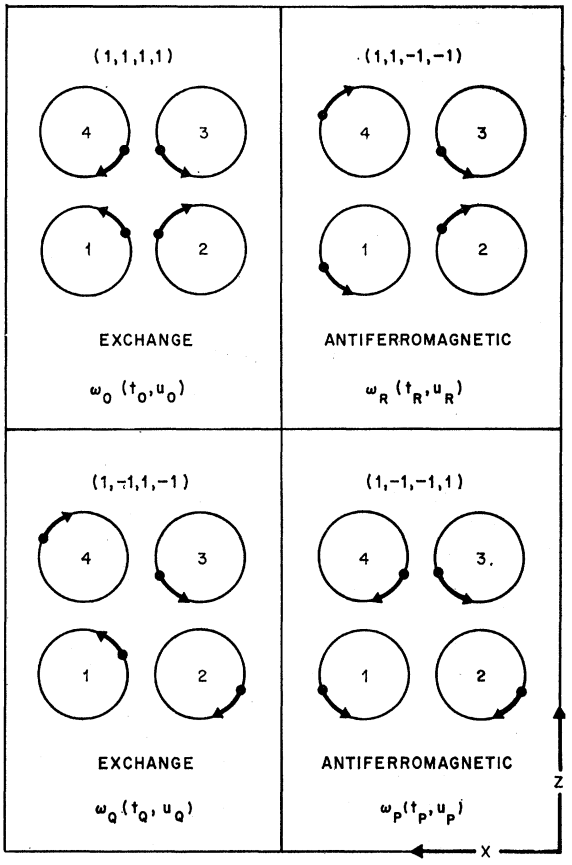

FIG. 3. Mode patterns of configuration I, showing idealized trajectories traced by magnetization vectors as viewed along the y axis, with vectors 1 and 3 pointing towards, and 2 and 4 away from the observer. The character with respect to $G_I \equiv E$, C_{2x}, C_{2y}, C_{2z}, the resonance frequency, and the precession coordinates are listed for each mode.

in these relations will be adhered to consistently in the remaining calculations. The free energy at equilibrium is

$$V=-4A_{yy}-(D_z+A_{xy})^2/E_R-(D_x-A_{yz})^2/E_P. \quad (7)$$

2. *Resonance Frequency*

There are 4 resonance modes corresponding to the symmetry characters (1,1,1,1), (1, 1, −1, −1), (1, −1, 1, −1), and (1, −1, −1, 1) of the group G_I. Idealized mode patterns are shown schematically in Fig. 3. By use of the symmetry coordinates introduced in Eq. (2) a separation of the dynamic equations is automatically obtained. First, one introduces a set of 4 distinct systems of coordinates (s_i,t_i,u_i), one for each sublattice, such that the s_i axis coincides with the equilibrium orientation of $\mathbf{r}_i$, and u_i is in the (x,y) plane. For sublattice 1 the transformation is given by

$$\begin{aligned} x_1&=s_1\sin\varphi\cos\theta-t_1\sin\varphi\sin\theta+u_1\cos\varphi,\\ y_1&=s_1\cos\varphi\cos\theta-t_1\cos\varphi\sin\theta-u_1\sin\varphi, \quad (8)\\ z_1&=s_1\sin\theta+t_1\cos\theta, \end{aligned}$$

where θ is the angle, at equilibrium, between $\mathbf{r}_1$ and the (x,y) plane, and φ the angle between the projection of $\mathbf{r}_1$ on the (x,y) plane and the y axis. According to (5) and (6), approximately

$$\varphi=(D_z+A_{xy})/2E_R, \quad (9)$$

$$\theta=-(D_x-A_{yz})/2E_P. \quad (10)$$

The coordinate systems for the remaining sublattices are chosen so as to give complete symmetry with respect to G_I, and the corresponding transformation equations are obtained by successively applying the operations of G_I to Eq. (8).

In the manner indicated in Eq. (2), one can combine the coordinates s_i, t_i, and u_i, into symmetry coordinates s_O, s_P, s_Q, s_R, etc. For these symmetry coordinates one obtains similar sets of transformations, the first of which is

$$\begin{aligned} x_O&=s_R\sin\varphi\cos\theta-t_R\sin\varphi\sin\theta+u_R\cos\varphi,\\ y_O&=s_Q\cos\varphi\cos\theta-t_Q\cos\varphi\sin\theta-u_Q\sin\varphi, \quad (11)\\ z_O&=s_P\sin\theta+t_P\cos\theta. \end{aligned}$$

The remaining transformations are obtained by successive application of the double-pair permutations $(OP)(QR)$, $(OQ)(PR)$, and $(OR)(PQ)$ to the subscripts in (11).

In order to obtain small signal equations for a weak rf magnetic field, $\mathbf{h}e^{i\omega t}$, Eqs. (4) must be expanded in terms of small deviations from equilibrium. At equilibrium itself $s_O=2$ and all other symmetry coordinates vanish. The simplest procedure is to first expand Eqs. (4) and then form the symmetry combinations in the fashion of Eq. (2). One obtains four separate sets of equations of the form

$$\begin{aligned} i\omega t_O&=-V_{Otu}t_O-(V_{Ouu}-V_s)u_O+h_{Ou}, \quad (12)\\ i\omega u_O&=(V_{Ott}-V_s)t_O+V_{Otu}u_O-h_{Ot}, \end{aligned}$$

with similar equations for the P, Q, and R components, where

$$V_s=\partial V/\partial s_i=\tfrac{1}{2}\partial V/\partial s_O,$$

and

$$V_{Otu}=\partial^2 V/\partial t_O\partial u_O, \quad V_{Ouu}=\partial^2 V/\partial u_O\partial u_O, \text{ etc.}$$

The derivatives are taken at equilibrium, and V, in these expressions, no longer includes the rf contribution from $\mathbf{h}$. The normal components of $\mathbf{h}$ are defined according to the standard procedure, indicated in (2), e.g.,

$$2h_{Ou}=h_{u1}+h_{u2}+h_{u3}+h_{u4},$$

where h_{ui} is the component of $\mathbf{h}$ along u_i. Using the transformation Eqs. (11) one finds

$$\begin{aligned} h_{Ou}&=0, & h_{Ot}&=0,\\ h_{Pu}&=0, & h_{Pt}&=2h_z\cos\theta, \quad (13)\\ h_{Qu}&=-2h_y\sin\varphi, & h_{Qt}&=-2h_y\cos\varphi\sin\theta,\\ h_{Ru}&=2h_x\cos\varphi, & h_{Rt}&=-2h_x\sin\varphi\sin\theta. \end{aligned}$$

Equation (12) is analogous to the equation for ferromagnetic precession of a single magnetization vector, and can be arrived at directly by noting that $V(u_i s_i t_i)$ is symmetric to double pair permutations of the indices and that all mixed derivatives of the form $\partial^2 V/\partial u_O \partial u_P$, etc., must vanish.

The formal solution of (12) is easily obtained. First one finds the resonance frequency by setting $\mathbf{h}=0$, giving

$$\omega_{\rm res}^2=(V_{tt}-V_s)(V_{uu}-V_s)-V_{tu}^2. \tag{14}$$

The solution of (12) is then given by

$$\begin{aligned} t&=(\omega_{\rm res}^2-\omega^2)^{-1}[(V_{uu}-V_s)h_t-(V_{tu}-i\omega)h_u],\\ u&=(\omega_{\rm res}^2-\omega^2)^{-1}[-(V_{tu}+i\omega)h_t+(V_{tt}-V_s)h_u], \end{aligned} \tag{15}$$

where the subscripts O, P, Q, R have been omitted, since the equations apply to each of the modes.

In order to obtain explicit expressions one must work out in detail all the coefficients which appear in Eq. (12) for the specific form of V. This requires first the substitution of (11) into (3), and then differentiation with respect to the symmetry coordinates. Within the approximation used here, one finds

$$\begin{aligned} &V_{Ott}-V_s=V_{Quu}-V_s=2E_P,\\ &V_{Ptt}-V_s=V_{Ruu}-V_s=2E_O,\\ &V_{Qtt}-V_s=V_{Ouu}-V_s=2E_R,\\ &V_{Rtt}-V_s=2(A_{yy}-A_{zz})+(D_z+A_{xy})^2/2E_R\\ &\qquad\qquad -2A_{yz}(D_x-A_{yz})/E_P,\\ &V_{Puu}-V_s=2(A_{yy}-A_{xx})+(D_x-A_{yz})^2/2E_P\\ &\qquad\qquad -2A_{xy}(D_z+A_{xy})/E_R,\\ &V_{Otu}=-D_{12y}+D_{14y}-A_{zx},\\ &V_{Ptu}=-D_y-A_{zx},\\ &V_{Qtu}=D_{12y}-D_{14y}-A_{zx},\\ &V_{Rtu}=D_y-A_{zx}. \end{aligned} \tag{16}$$

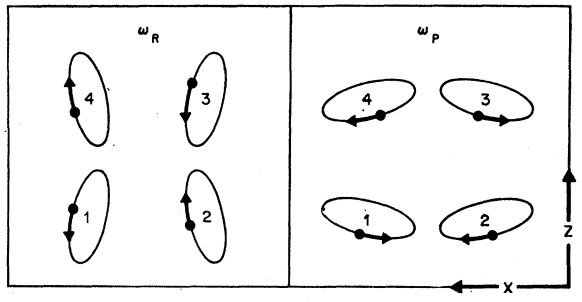

FIG. 4. Schematic trajectories in the antiferromagnetic modes of configuration I.

In the same approximation, the resonances are given by

$$\begin{aligned} &\omega_O^2\simeq\omega_Q^2\simeq 4E_PE_R,\\ &\omega_P^2=4E_O[(A_{yy}-A_{xx})+(D_x-A_{yz})^2/4E_P\\ &\qquad +A_{xy}(D_z+A_{xy})/E_R]-(D_y+A_{zx})^2,\\ &\omega_R^2=4E_O[(A_{yy}-A_{zz})+(D_z+A_{xy})^2/4E_R\\ &\qquad -A_{yz}(D_x-A_{yz})/E_P]-(D_y-A_{zx})^2. \end{aligned} \tag{17}$$

ω_O^2 and ω_Q^2 are not strictly identical, their relative difference being of the order of the square of the canting angle. The precession amplitudes are

$$\begin{aligned} t_P&=\frac{\omega_P^2+(D_y+A_{zx})^2}{(\omega_P^2-\omega^2)E_O}h_z,\\ u_P&=\frac{2(D_y+A_{zx}-i\omega)}{\omega_P^2-\omega^2}h_z,\\ t_Q&=\frac{2(D_x-A_{yz})}{\omega_Q^2-\omega^2}h_y,\\ u_Q&=-\frac{2(D_z+A_{xy})}{\omega_Q^2-\omega^2}h_y,\\ t_R&=-\frac{2(D_y-A_{zx}-i\omega)}{\omega_R^2-\omega^2}h_x,\\ u_R&=\frac{\omega_R^2+(D_y-A_{zx})^2}{(\omega_R^2-\omega^2)E_O}h_x. \end{aligned} \tag{18}$$

The optical activities of the P, Q, and R modes are, respectively, along z, y, and x directions. The O mode is inactive. P and R are antiferromagnetic modes, O and Q exchange modes with much higher resonance frequencies. The eliptic trajectories of the antiferromagnetic modes are highly eccentric (Fig. 4), the ratio of minor to major axis being of the order of ω_P/E_O or ω_R/E_O, and the optical activity is confined to the direction of the minor axis.

3. *Susceptibility*

The total magnetization is $\sum \mathbf{M}_i=M\sum \mathbf{r}_i=2M\mathbf{r}_O$. The rf components of $\mathbf{r}_O$ are expressed in terms of the normal mode coordinates by Eq. (11), in which the terms containing s coordinates are left out. With the help of Eqs. (18), (9), and (10) one readily obtains the coefficients of the susceptibility tensor,

$$\begin{aligned} &\chi_{xx}=(2M/E_O)[\omega_R^2+(D_y-A_{zx})^2]/(\omega_R^2-\omega^2),\\ &\chi_{yy}=2M[(D_x-A_{yz})^2/E_P+(D_z+A_{xy})^2/E_R]/(\omega_Q^2-\omega^2),\\ &\chi_{zz}=(2M/E_O)[\omega_P^2+(D_y+A_{zx})^2]/(\omega_P^2-\omega^2). \end{aligned}$$

By setting $\omega=0$ one obtains the dc susceptibility

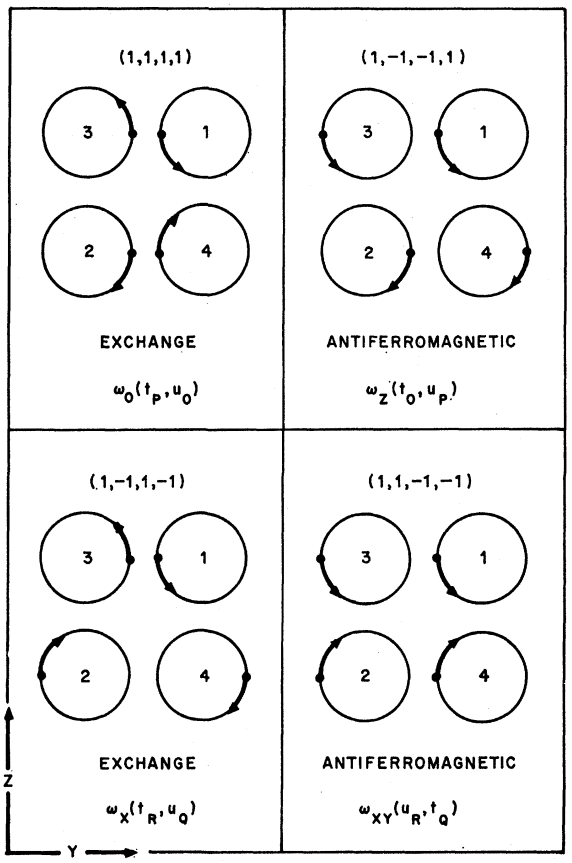

FIG. 5. Approximate mode patterns of configuration IV, as viewed along the x axis, with trajectories of vectors 1 and 3 displayed above those of 2 and 4. The character is with respect to $G_{IV}=E$, RC_{2x}, RC_{2y}, C_{2z} where time reversal is assumed to occur when the z component of precession vanishes. The precession coordinates listed are not true normal coordinates.

coefficients

$$\chi_{xx}(\omega=0)=(2M/E_O)[1+(D_y-A_{zz})^2/\omega_R{}^2],$$
$$\chi_{yy}(\omega=0)=(2M/\omega_Q{}^2)[(D_x-A_{yz})^2/E_P+(D_z+A_{xy})^2/E_R],$$
$$\chi_{zz}(\omega=0)=(2M/E_O)[1+(D_y+A_{zz})^2/\omega_P{}^2].$$

4. "Screw" Susceptibility

The expressions for χ_{xx} and χ_{zz} are surprising at first sight. Intuitively, one would expect the four magnetization vectors to bend toward a magnetic field which is applied essentially at right angles to their orientation. The field would thus be acting directly against the antiferromagnetic exchange field E_O, and in the present approximation this would lead to the usual susceptibility values in antiferromagnets, namely $\chi_{xx}=\chi_{zz}=2M/E_O$.

To arrive at a physical explanation for this apparent discrepancy, let us consider the geometric meaning of the coordinates t_P, u_P, t_R, u_R. From the definitions one sees that t_P and u_R represent bending of all magnetization vectors towards z and x, respectively, whereas u_P and t_R represent rigid rotations about these axes. From (18) it is evident that the rotational coordinates u_P and t_R are large compared to their bending counterparts, t_P and u_R. The application of a magnetic field in a direction perpendicular to y thus results in a screw motion consisting of a large rotation about the field accompanied with slight bending towards the field. (The sense of the rotation will depend on the domain type.) The rotation indicates an inclination of configuration I to go over into configuration II or IV, which upon application of a field, become energetically more favorable on account of their residual magnetism. The incremental magnetization appearing in Eq. (20) is thus accounted for by an admixture from configurations II and IV which is introduced upon applying a magnetic field.

Configuration IV

The treatment of configuration IV follows that of configuration I in many details, and it will save space if we apply an essentially identical notation to the present case. To avoid confusion we must stress at the outset that equations and definitions used in this section apply exclusively to configuration IV.

The difficulties in the treatment of configuration IV are due to the presence of time-reversing elements in the magnetic group. The group $G_{IV}\equiv E$, $RC_x(14)(23)$, $RC_y(13)(24)$, $C_z(12)(34)$ is isomorphic to D_2 and has the same character table as G_I. The characterization of normal modes according to this table is, however, not in general possible *a priori*, because of the nonunitary properties of R (see Wigner[14] for a discussion of this point. Physically the ambiguity lies in specifying the exact instant of time reversal relative to the precession phase). The characterization and separation of modes is therefore more complicated in the present case.

1. Equilibrium Position and Energy

The only nonvanishing symmetry coordinates at equilibrium are x_Q, y_R, and z_O. The spins lie essentially along the x direction, hence $x_Q\simeq 2$, and to first order

$$y_R=(D_z-A_{xy})/E_R, \quad (21)$$
$$z_O=(D_y+A_{xz}+H)/E_O, \quad (22)$$

where H is an applied constant field along the z direction.

There is a residual net magnetization along z, given by

$$|\sum \mathbf{M}_i|=2Mz_O=(2M/E_O)(D_y+A_{xz}). \quad (23)$$

The free energy at equilibrium, to first order, is

$$V=-4A_{xx}-(D_y+A_{xz}+H)^2/E_O-(D_z-A_{xy})^2/E_R. \quad (24)$$

2. Resonance Frequencies

The precession modes can be classified according to the characters (1,1) or (1, −1) with respect to the subgroup E, $C_{2z}(12)(34)$. Further classification with respect to $RC_{2x}(14)(23)$ and $RC_{2y}(13)(24)$ is ambiguous

[14] E. Wigner, *Group Theory and its Application to the Quantum Mechanics of Atomic Spectra*, (Academic Press, Inc., New York).

since it depends on the choice of the exact instant at which precession is reversed. Nonetheless, one gains physical insight by considering the approximate mode patterns presented in Fig. 5, in which time reversal is defined as occurring at the instant at which all z components of the precession vanish. (This approximation is closely related to the 2-sublattice model.) The resonances are designated as ω_0, ω_x, ω_{xy}, and ω_z, where the subscripts refer to the direction of optical activity of the modes, in this approximation. ω_0 and ω_x represent exchange modes and ω_{xy} and ω_z antiferromagnetic modes. The detailed calculation shows that these modes are not normal, as each antiferromagnetic mode is coupled to an exchange mode, and that, as a result, the optical activity is not confined to the directions specified.

We proceed again by introducing 4 separate coordinate systems, $(s_i t_i u_i)$ where s_i is along $\mathbf{r}_i$ at equilibrium, and u_i is in the (x,y) plane. The transformations for r_1 are

$$\begin{aligned} x_1&=s_1\cos\varphi\cos\theta-t_1\cos\varphi\sin\theta-u_1\sin\varphi,\\ y_1&=-s_1\sin\varphi\cos\theta+t_1\sin\varphi\sin\theta-u_1\cos\varphi,\\ z_1&=s_1\sin\theta+t_1\cos\theta, \end{aligned} \tag{25}$$

where θ is the angle between $\mathbf{r}_1$ at equilibrium with the (x,y) plane and φ the angle which the projection of $\mathbf{r}_1$ on the (x,y) plane makes with the x axis. According to (21) and (22)

$$\begin{aligned} \varphi&\simeq(D_z-A_{xy})/2E_R,\\ \theta&\simeq(D_y+A_{zx}+H)/2E_O. \end{aligned} \tag{26}$$

The remaining transformations are obtained by successively applying to (24) the symmetry operations of G_{IV}. The effect of the time-reversal elements is to make the coordinate systems for sublattices 2 and 3 left handed. For the symmetry coordinates the appropriate transformations are

$$\begin{aligned} x_O&=s_Q\cos\varphi\cos\theta-t_Q\cos\varphi\sin\theta-u_Q\sin\varphi,\\ y_O&=-s_R\sin\varphi\cos\theta+t_R\sin\varphi\sin\theta-u_R\cos\varphi,\\ z_O&=s_O\sin\theta+t_O\cos\theta, \end{aligned} \tag{27}$$

where the remaining transformations are again obtained by successive application of the permutations $(OP)(QR)$, $(OQ)(PR)$, and $(OR)(PQ)$.

The small signal equations are obtained as in configuration I. In the coordinate systems (s_2,t_2,u_2) and (s_3,t_3,u_3) there is, however, a sign reversal associated with taking the time derivative. Hence, when forming standard linear combinations of the equations, one obtains expressions of the P, O, R, Q, on the left side of the equations, opposite expressions of the form O, P, Q, R, respectively, on the right. There are therefore two systems of coupled equations, the first being

$$\begin{aligned} i\omega t_O&=-V_{Ptu}t_P-(V_{Puu}-V_s)u_P+h_{Pu},\\ i\omega u_O&=(V_{Ptt}-V_s)t_P+V_{Ptu}u_P-h_{Pt},\\ i\omega t_P&=-V_{Otu}t_O-(V_{Ouu}-V_s)u_O+h_{Ou},\\ i\omega u_P&=(V_{Ott}-V_s)t_O+V_{Otu}u_O-h_{Ot}. \end{aligned} \tag{28}$$

The second set is obtained by applying $(OQ)(PR)$. The components of h are given by

$$\begin{aligned} h_{Ot}&=2h_z\cos\theta, & h_{Ou}&=0,\\ h_{Pt}&=0, & h_{Pu}&=0,\\ h_{Qt}&=-2h_x\cos\varphi\sin\theta, & h_{Qu}&=-2h_x\sin\varphi,\\ h_{Rt}&=2h_y\sin\varphi\sin\theta, & h_{Ru}&=-2h_y\cos\varphi. \end{aligned} \tag{29}$$

Equation (28) can be interpreted as coupling an antiferromagnetic mode with coordinates (t_O,u_P) to an exchange mode with coordinates (t_P,u_O) via the coefficients V_{Otu} and V_{Ptu}.

In order to solve (28), one first puts it in the form of a "Telegraphy Equation." Defining

$$\psi=\begin{bmatrix} t_O\\ u_O\\ t_P\\ u_P \end{bmatrix},\qquad \eta=\begin{bmatrix} h_{Pu}\\ -h_{Pt}\\ h_{Ou}\\ -h_{Ot} \end{bmatrix}$$

and

$$\mathbf{T}=\begin{bmatrix} 0 & 0 & -V_{Ptu} & -(V_{Puu}-V_s)\\ 0 & 0 & (V_{Ptt}-V_s) & V_{Ptu}\\ -V_{Otu} & -(V_{Ouu}-V_s) & 0 & 0\\ (V_{Ott}-V_s) & V_{Otu} & 0 & 0 \end{bmatrix},$$

one can write (28) in the matrix form $i\omega\psi=\mathbf{T}\psi+\eta$. By substituting the right-hand into the left-hand side of the equation, one obtains

$$(\omega^2+\mathbf{T}^2)\psi=-(\mathbf{T}+i\omega)\eta, \tag{30}$$

with

$$\mathbf{T}^2=\begin{bmatrix} -k & m & 0 & 0\\ n & -l & 0 & 0\\ 0 & 0 & -l & -m\\ 0 & 0 & -n & -k \end{bmatrix},$$

where

$$\begin{aligned} k&=(V_{Puu}-V_s)(V_{Ott}-V_s)-V_{Otu}V_{Ptu},\\ l&=(V_{Ouu}-V_s)(V_{Ptt}-V_s)-V_{Otu}V_{Ptu},\\ m&=V_{Ptu}(V_{Ouu}-V_s)-V_{Otu}(V_{Puu}-V_s),\\ n&=V_{Ptu}(V_{Ott}-V_s)-V_{Otu}(V_{Ptt}-V_s). \end{aligned} \tag{31}$$

Equation (30) separates into two independent sets of equations for (u_O,t_O) and for (u_P,t_P). The resonance frequencies are obtained from the secular equation

$$\mathrm{Det}(\omega_{res}^2+\mathbf{T}^2)=0,$$

which gives

$$(\omega_{res}^2-k)(\omega_{res}^2-\ell)=mn$$

with solutions

$$\omega_{res}^2=\tfrac{1}{2}(\ell+k)\pm\tfrac{1}{2}[(\ell-k)^2+4mn]^{1/2}.$$

Since, in our case $4mn\ll(\ell-k)^2$, one obtains the following approximate expressions for the two resonance frequencies denoted ω_0 and ω_z:

$$\begin{aligned}\omega_0^2&=\ell+mn/(\ell-k),\\ \omega_z^2&=k-mn/(\ell-k).\end{aligned}\tag{32}$$

In complete analogy one obtains two additional resonances ω_x and ω_{xy} from the equation for the Q and R coordinates. An approximate assignment of coordinates to each resonance mode is given in Fig. 5.

A detailed calculation of the coefficients appearing in (28) gives, to first order,

$$\begin{aligned}&V_{Ott}-V_s=V_{Ruu}-V_s=2E_O,\\ &V_{Ptt}-V_s=V_{Quu}-V_s=2E_P,\\ &V_{Rtt}-V_s=V_{Ouu}-V_s=2E_R,\\ &V_{Qtt}-V_s=2(A_{xx}-A_{zz})+(4A_{zz}+H)(D_y+A_{zx}+H)/2E_O+(D_z-A_{xy})^2/2E_R,\\ &V_{Puu}-V_s=2(A_{xx}-A_{yy})+(D_y+A_{zx})\times(D_y+A_{zx}+H)/2E_O-2A_{xy}(D_z-A_{xy})/2E_R,\\ &V_{Otu}=-A_{yz}-D_{12x}-D_{13x},\\ &V_{Ptu}=-D_x-A_{yz},\\ &V_{Qtu}=D_x-A_{yz},\\ &V_{Rtu}=D_{12x}+D_{13x}-A_{yz}.\end{aligned}\tag{33}$$

From Equations (32), and their analogs for ω_x^2 and ω_{xy}^2, one obtains, after proper substitutions and approximations,

$$\begin{aligned}&\omega_0^2\simeq\omega_x^2\simeq4E_PE_R,\\ &\omega_{xy}^2=4E_O[(A_{xx}-A_{zz})+(D_z-A_{xy})^2/4E_R-(D_x-A_{yz})^2/4E_P]+(4A_{zz}+H)(D_y+A_{zx}+H),\\ &\omega_z^2=4E_O[(A_{xx}-A_{yy})-A_{xy}(D_z-A_{xy})/E_R-(D_x+A_{yz})^2/4E_P]+(D_y+A_{zz})(D_y+A_{zx}+H),\end{aligned}\tag{34}$$

where again ω_0^2 and ω_x^2 differ by a relative amount of the order of the square of canting angles.

To obtain the precession amplitudes one must solve (30) in detail for all modes. Because of their length we will not reproduce the expressions in full, but confine ourselves to some general remarks. Each precession coordinate contains a direct resonance term and a mode interaction term. For example, the coordinates t_O and u_P which belong with ω_z, have a direct term proportional to $(\omega_z^2-\omega^2)^{-1}$, and a term proportional to $(\omega_z^2-\omega^2)^{-1}(\omega_0^2-\omega^2)^{-1}$ which results from the coupling to the ω_0 exchange mode. The eliptic trajectories associated with the antiferromagnetic modes are highly eccentric, the ratio of minor to major axis being of the order of ω_z/E_O and ω_{xy}/E_O, respectively. These are represented schematically in Fig. 6. The tilting of the elipses is due to the interaction with exchange modes.

3. *Susceptibility*

As in configuration I the susceptibility is obtained from $\sum\mathbf{M}_i=2M\mathbf{r}_O$, where $\mathbf{r}_O$ is given in terms of the mode coordinates according to Eq. (27), with the s coordinates left out. A detailed and somewhat lengthy calculation gives

$$\begin{aligned}\chi_{xx}&=2M\left[\frac{(D_y+A_{zx}+H)^2}{(\omega_{xy}^2-\omega^2)E_O}+\frac{(D_z-A_{xy})^2}{(\omega_x^2-\omega^2)E_R}\right],\\ \chi_{xy}&=-\chi_{yx}^*=2i\omega M\left[\frac{(D_y+A_{zx}+H)}{(\omega_{xy}^2-\omega^2)E_O}-\frac{2(D_x-A_{yz})(D_z-A_{xy})}{(\omega_{xy}^2-\omega^2)(\omega_x^2-\omega^2)}\right],\\ \chi_{yy}&=2M\left[\frac{\omega_{xy}^2}{(\omega_{xy}^2-\omega^2)E_O}-\frac{2\omega^2(D_x-A_{yz})^2}{(\omega_{xy}^2-\omega^2)(\omega_x^2-\omega^2)E_P}\right],\\ \chi_{zz}&=2M\left[\frac{\omega_z^2}{(\omega_z^2-\omega^2)E_O}-\frac{2\omega^2(D_x+A_{yz})^2}{(\omega_z^2-\omega^2)(\omega_0^2-\omega^2)E_P}\right].\end{aligned}\tag{35}$$

In order to obtain the dc susceptibilities one sets $\omega=0$ and substitutes $h_x\rightarrow H_x$, $h_y\rightarrow H_y$, $h_z\rightarrow H_z$, $H\rightarrow H_z$, and expands up to quadratic terms in the fields. One then obtains

$$\begin{aligned}\chi_{xx}(\omega=0)&=2M(D_y+A_{xz})^2/\omega_{xy}^2E_O,\\ \chi_{yy}(\omega=0)&=\chi_{zz}(\omega=0)=2M/E_O,\end{aligned}\tag{36}$$

for the linear coefficients, and

$$C_{xxz}=[2M(D_y+A_{xz})/E_O\omega_{xy}^4]\times[2\omega_{xy}^2-(D_y+A_{zx})(D_y+5A_{zx})],\tag{37}$$

for the quadratic coefficient. The frequency ω_{xy} in (36) and (37) is taken from (34) for $\mathbf{H}=0$.

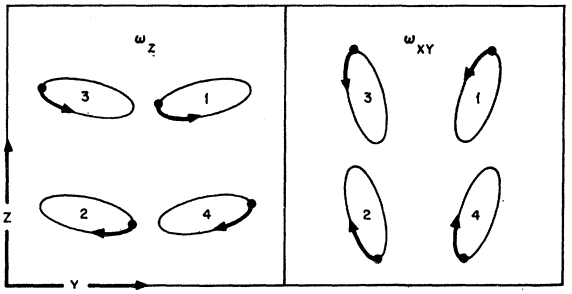

FIG. 6. Schematic trajectories in the antiferromagnetic modes of configuration IV.

Configuration II

It will be observed that Eqs. (1) and (3) are invariant to a transformation consisting of (1) interchanging x and z, (2) interchanging the subscripts 2 and 4, (3) interchanging the subscripts P and R, (4) reversing the sign of all D coefficients, and (5) reversing the sign of all coordinates. This transformation effects a complete mapping of configuration II and everything relating to it into configuration IV. All equations of the last section can be systematically transformed to give the analogous equations for configuration II, and there is no need to treat this configuration separately.

The study of configuration II is of practical interest even in those cases where configuration IV is the normal ground state, since the application of a sufficiently high field along the z direction may cause the magnetization vectors to flip from the latter to the former. The stability condition for configuration II under those circumstances is that the frequency ω_{yz} be real (the reality of ω_z will usually follow automatically), or,

$$\omega_{yz}^2=4E_O[(A_{zz}-A_{xx})+(D_x+A_{yz})^2/4E_P-(D_z+A_{xy})^2/4E_R]+(-4A_{xz}+H)(D_z-A_{xz}+H)>0. \quad (38)$$

For fields slightly above the flipping field, H_F,

$$\omega_{yz}^2\simeq(D_z-5A_{xz}+2H_F)(H-H_F). \quad (39)$$

This mode is therefore distinguished by its low frequency, and its tremendous sensitivity to small changes in the magnetic field.

IV. DISCUSSION

At first sight it would seem that all of the results obtained in the last section show a clear dependence on hidden as well as overt canting parameters. A closer look will show that at low frequencies (i.e., low compared to the exchange resonances) the dependence on the hidden parameters is largely formal. This becomes most apparent when $A\ll D$, (which, according to Treves,[9] is probably the rule in most orthoferrites) in which case one may neglect the off-diagonal terms of A. One can then introduce effective anisotropy constants given by

$$\begin{aligned}\bar{A}_{xx}&=A_{xx}+D_z^2/4E_R,\\ \bar{A}_{yy}&=A_{yy}=D_z^2/4E_R+D_x^2/4E_P,\\ \bar{A}_{zz}&=A_{zz}+D_x^2/4E_P,\end{aligned} \quad (40)$$

which completely account for the effect of the hidden canting parameters, as can be seen by substituting (40) into (7), (24), (17), and (34) (and the corresponding equations for structure II), as well as into the susceptibility expressions at low frequencies. The antiferromagnetic resonances, and the low-frequency behavior in general can in this case be completely described in terms of a 2-sublattice model, which is obtained by lumping together $\mathbf{M}_1$ and $\mathbf{M}_3$, and $\mathbf{M}_2$ and $\mathbf{M}_4$. The results obtained here in fact agree completely with those obtained for the 2-sublattice model in an earlier work,[10] provided $\bar{A}_{xx}$, $\bar{A}_{yy}$ and $\bar{A}_{zz}$ are substituted for A_{xx}, A_{yy} and A_{zz}. It must, however, be stressed that the model is strictly formal, not physical. The effective anisotropy may bear little relation to the spin Hamiltonian in an analogous paramagnetic configuration and its temperature dependence must reflect the contribution of hidden exchange parameters.

When $A\ll D$ does not hold, it is in general impossible to introduce a 2-sublattice model which will account consistently for all relations. But in this case too, the hidden canting parameters are always found in combination with anisotropy constants and cannot be separately extracted from the macroscopic data at low frequencies.

Clearcut evidence for hidden canting must be sought in the behavior of the high-frequency exchange modes. In configuration IV, the ω_0 mode is optically active in the z direction and the ω_x mode is active also in the y direction. This activity results entirely from hidden canting.

The total number of measurable parameters is thus rather small. E_O, D_y, and A_{xz} can be obtained from measurement of the residual magnetization, the dc susceptibility, and the field dependence of antiferromagnetic resonance. From these resonances one also obtains effective anisotropy constants whose physical nature is complex. The exchange frequencies yield the product E_PE_R, the absolute line strength measurements of these resonances in configurations II and IV yield the parameters $(D_z\pm A_{xy})^2/E_R$ and $(D_x\pm A_{yz})^2/E_P$.

The optical activity of the resonance modes is rather weak. If one takes as a standard the susceptibility near resonance of a ferromagnet with magnetization $4M$, i.e.,

$$4M\omega_{\rm res}/(\omega_{\rm res}^2-\omega^2),$$

then the strength of the antiferromagnetic modes is weaker by a factor of the order of $\omega_{\rm res}/E_O$, which is generally comparable to a canting angle, and the strength of exchange modes weaker by the order of D^2/E^2 or roughly the square of a canting angle.

Some cautionary remarks are called for concerning certain approximations and assumptions used. These are

(1) Neglecting of symmetric anisotropic exchange. Such terms become submerged in the single-ion anisotropy term.

(2) Neglecting higher than quadratic terms in the anisotropy. At room temperatures this assumption is probably justified on the basis of paramagnetic resonance data, but at low temperature the effect of higher terms could be significant.

All of these considerations combine to indicate, that in the expressions of the previous section one should regard the anisotropy constants as describing the anisotropy surface only in the neighborhood of each par-

ticular equilibrium position. The effective local anisotropy thus contains in addition to hidden canting contributions also contributions from anisotropic exchange and higher-order terms of the single-ion anisotropy. This can result in a complicated temperature dependence and considerable caution is required in applying a physical interpretation to the data.

V. CONCLUSION

A complete derivation of the resonances and susceptibilities has been presented, for the various possible magnetic ground states in orthoferrites. The results show a dependence not only on overt canting but also on the hidden canting mechanism. When the anisotropy energy is small compared to the antisymmetric exchange, it is possible to describe the low-frequency behavior on the basis of a formal 2-sublattice model, employing an effective anisotropy energy which includes hidden contributions of an exchange character. At low frequencies hidden canting cannot be observed directly, but its indirect effect may be noticed in the temperature dependence of measured parameters.

The chief observable effects associated with hidden canting is the susceptibility of the exchange resonances. In a purely antiferromagnetic configuration these modes would be optically inactive. Hidden canting introduces a coupling between exchange modes and antiferromagnetic modes, which result in optical activity of the former.

In general, one may conclude, that out of the large number of coefficients which play a role in the interactions among the four magnetic sublattices, only relatively few are susceptible to macroscopic observation.

ACKNOWLEDGMENT

This work was initiated while the author was at General Telephone and Electronics Laboratories, Palo Alto, California.

PHYSICAL REVIEW VOLUME 133, NUMBER 5A 2 MARCH 1964

Low-Temperature Behavior of a Face-Centered Cubic Antiferromagnet

A. DANIELIAN*
Wheatstone Physics Laboratory, University of London King's College, London, England
(Received 7 October 1963)

A detailed description of the ground state of a face-centered cubic antiferromagnetic system with Ising interactions is followed by an investigation of the low-temperature thermodynamic properties by means of a power series expansion of the partition function about $T=0°K$. This expansion has been found to be possible even though the ground state is degenerate because of the existence of a substantial amount of "partial long-range order." Expressions for the zero-field magnetic susceptibility and the specific heat are derived.

INTRODUCTION

THE low-temperature thermodynamic properties of magnetic spin systems with Ising interactions have been investigated by means of series expansions (for a review, see Ref. 1). The general principle is that at low temperatures the partition function can be expanded in terms of successive deviations ('excited states') from an ordered ground state. This has not hitherto been possible in the case of a face-centered cubic system, because it does not have an ordered ground state when nearest-neighbor interactions only are present. In a previous communication,[2] the present author determined the degeneracy of the ground state of such a system and gave a complete classification of the ground-state configurations. As a result it is found that, although the ground state is degenerate, there exists a substantial amount of "partial long-range order" which makes it possible for the partition function to be expanded in the usual manner to a limited number of terms. In the following section the ground state of the face-centered cubic system is discussed further; subsequently some of the excited states are evaluated and expressions for the zero-field magnetic susceptibility and specific heat derived.

II. THE GROUND STATE

We first give a summary of the results reported in Ref. 2 concerning the ground state of a face-centered cubic antiferromagnetic system of N spin moments each having two possible states ($\pm$). First, the energy of the ground state is $-2NJ$, where $+J$ is the interaction energy between neighboring parallel spins ($++$, $--$) and $-J$ the interaction energy between neighboring antiparallel spins ($+-$). Second, the configurational state of any one triangular layer of the lattice determines uniquely the configurational state of the whole

* Present address: Department of Physics, University of Toronto, Toronto, Ontario, Canada.
[1] C. Domb, Phil. Mag. 9, Suppl. 34, 149 (1960).
[2] A. Danielian, Phys. Rev. Letters 6, 670 (1961).